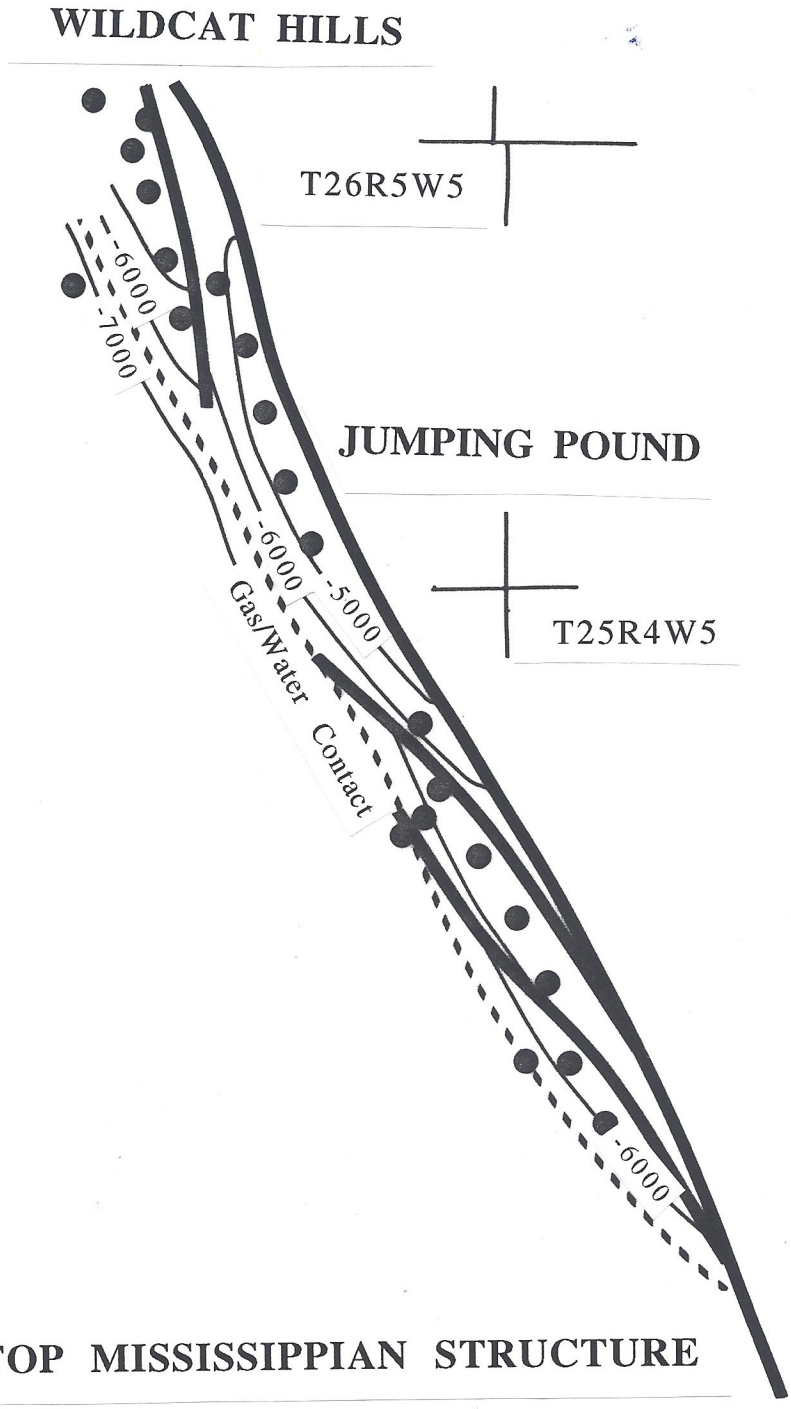

TOP MISSISSIPPIAN STRUCTURE

THRUST FAULT LINKAGE

&

CONSIDERATIONS FOR TRAP INTEGRITY

Dave Klepacki
March 7, 1994

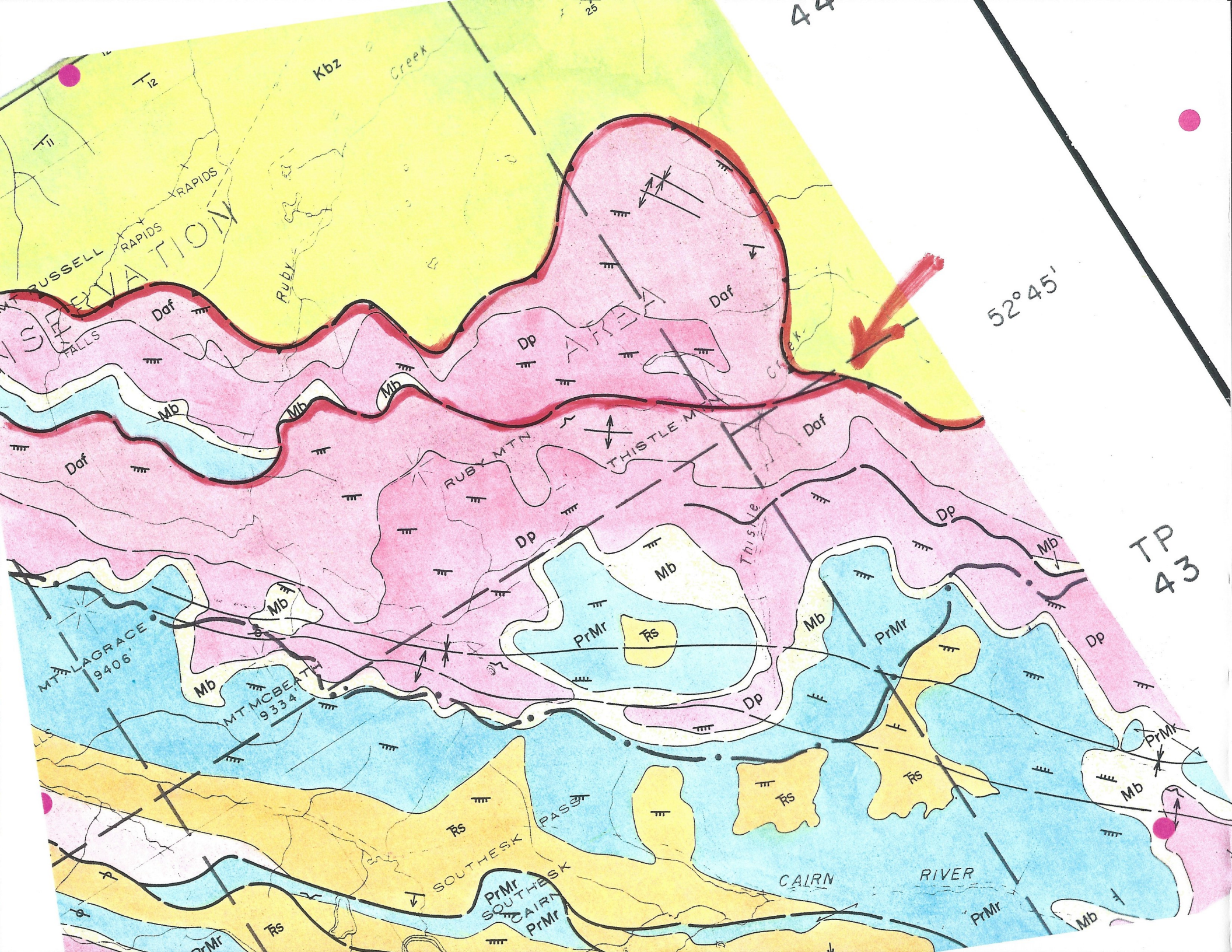
44
52°45'
TP
43
Kbz
Creek
RAPIDS
RUSSELL
RAPIDS
RUBY
Daf
Dp
Mb
RUBY MTN
THISTLE
Thistle
PrMr
Rs
MT ALAGRACE
9406'
MT MCBEATH
9334'
SOUTHESK PASS
SOUTHESK
CAIRN
RIVER
CAIRN
PrMr

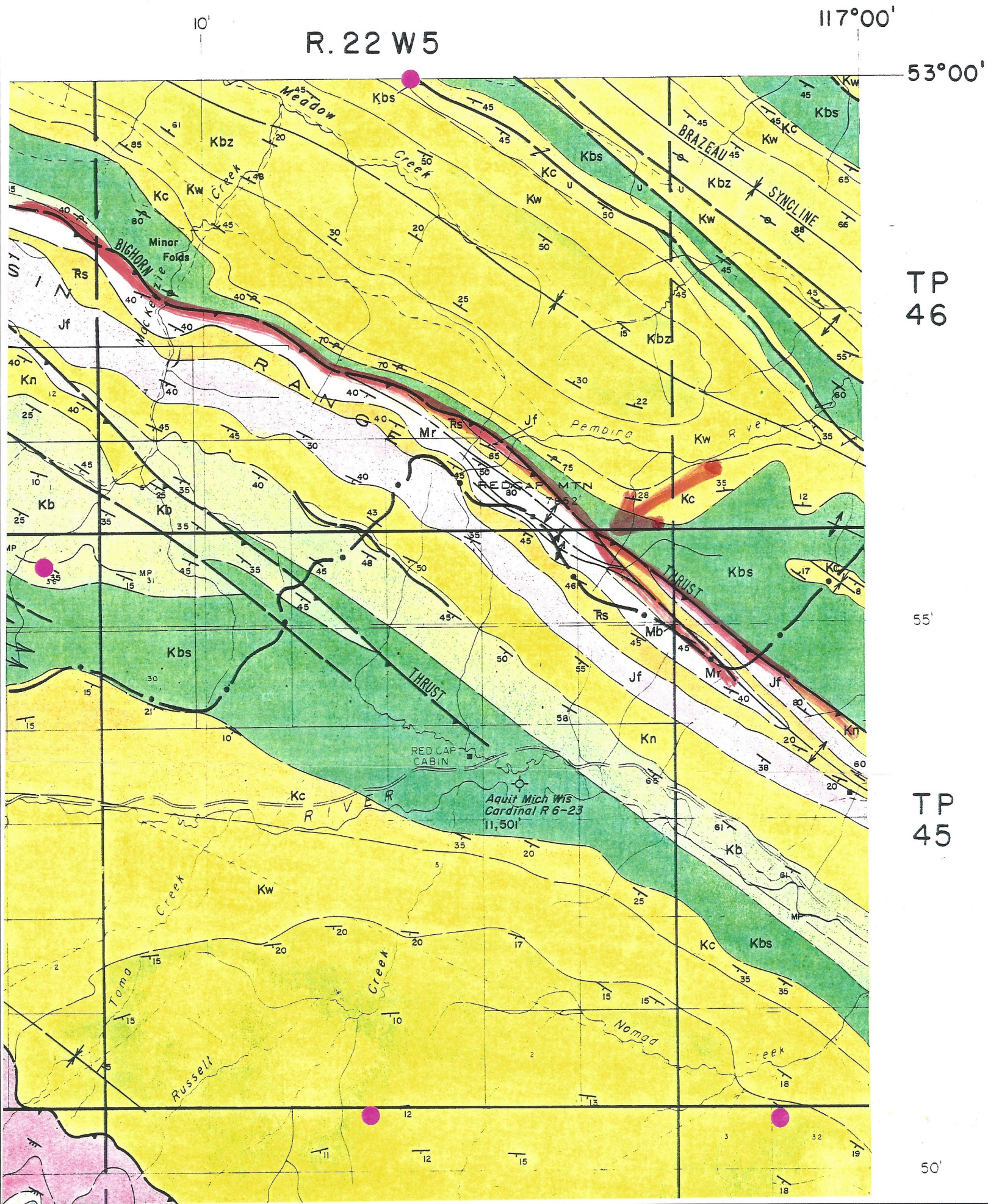
10'
R. 22 W5
117°00'
53°00'
Meadow Creek
Kbs
Kbz
Kc
Kw
Creek
BRAZEAU SYNCLINE
Minor Folds
BIGHORN
Mackenzie
Rs
Jf
Kn
RANGE
Mr
Pembina River
REDCAP MTN
Kb
THRUST
Mb
RED CAP CABIN
Aquit Mich Wis
Cardinal R 6-23
11,501'
Toma Creek
Russell Creek
Nomgd Creek
TP 46
TP 45
55'
50'


-2669
-2431
-2229
-2450
-2426
-1897
-2159
-2877
-1688
-2705

"AS THE INITIAL BREAKS DEVELOPED INTO THRUSTS, NEW ONES FORMED AND EVENTUALLY THE VARIOUS EXTENSIONS OF THE THRUSTS INTERLOCKED, MERGED, OR SUBSIDIARY CONNECTING FAULTS FORMED BETWEEN THEM."

R.J.W. Douglas, 1958, Mount Head Map-Area, Alberta. Geological Survey of Canada Memoir 291, p.131.

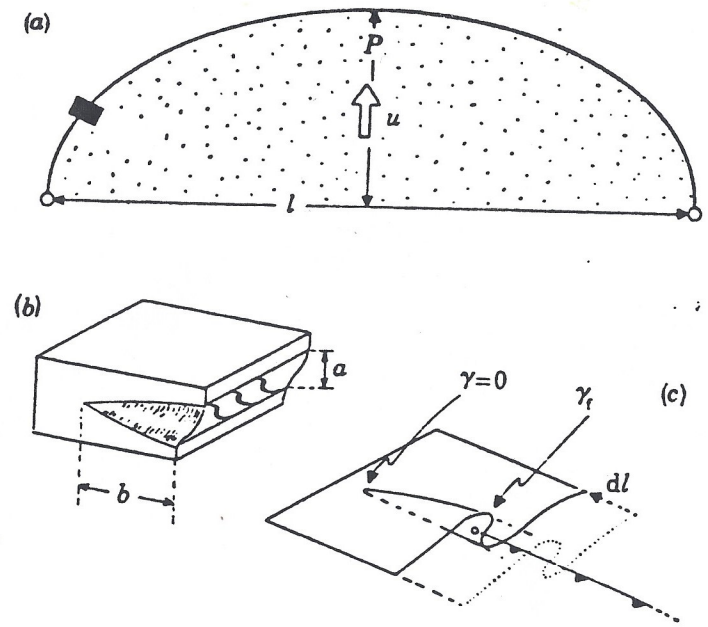

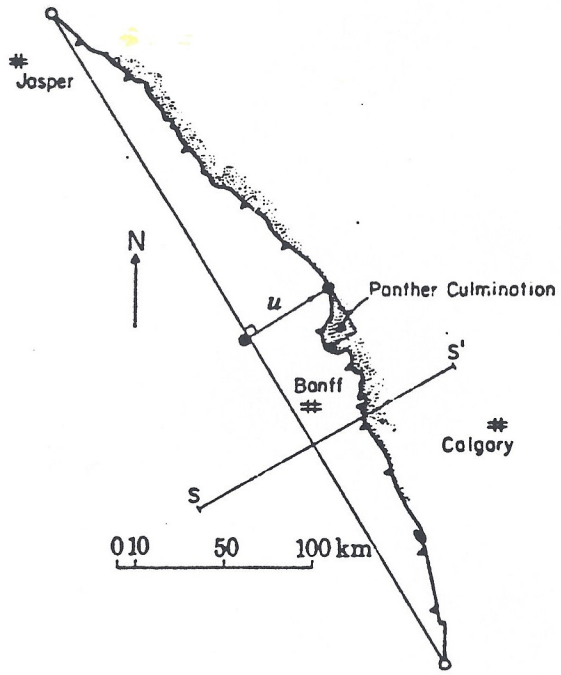

Elliot, D, 1976, The energy balance and deformation mechanisms of thrust sheets. Phil. Trans. R. Soc. London, A283: p 289-312.

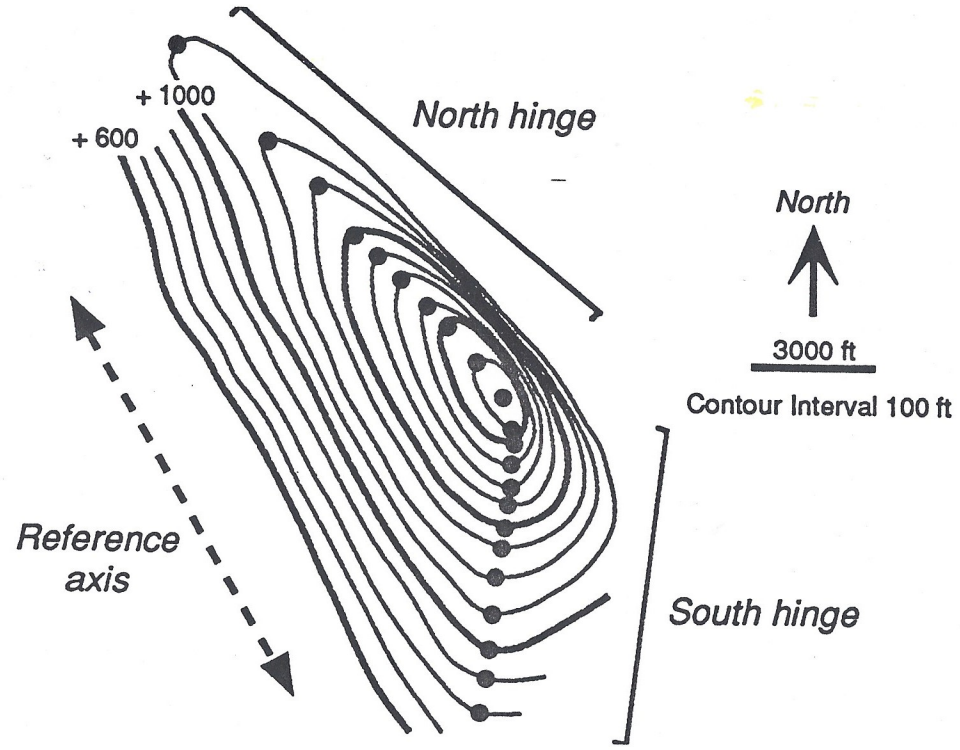

Figure 15. Loci of points defining north and south hinge lines of Frannie fold, Park County, Wyoming (WGA 1989). North hinge appears to represent boundary between forelimb and backlimb domains; south hinge corresponds to crest-backlimb boundary.

Ratliff, R.A., 1994, Three-Dimensional Fault-Propagation Folding: a Model Based on Displacement Variation. Journal of Structural Geology.

linear-arithmetic, $$d = a + b\left[1 - \left(\frac{r}{c}\right)^{3/2}\right]\left[1 - \left(\frac{2r}{r+c}\right)^{2}\right]^{1/2}; \quad (12)$$

constant-arithmetic, $$d = a + 2b\left(1 - \frac{r}{c}\right)\left[\left(\frac{1+\frac{r}{c}}{2}\right)^{2} - \left(\frac{r}{c}\right)^{2}\right]^{1/2}; \quad (13)$$

cosinusoidal, $$d = a + \frac{b}{2}\left[1 + \cos\left(\frac{\pi r}{c}\right)\right]; \quad (14)$$

elliptical, $$d = a + \left[b^{2} - \left(\frac{br}{c}\right)^{2}\right]^{1/2}; \quad (15)$$

and parabolic, $$d = a + b\left[1 - \left(\frac{r}{c}\right)^{2}\right]. \quad (16)$$

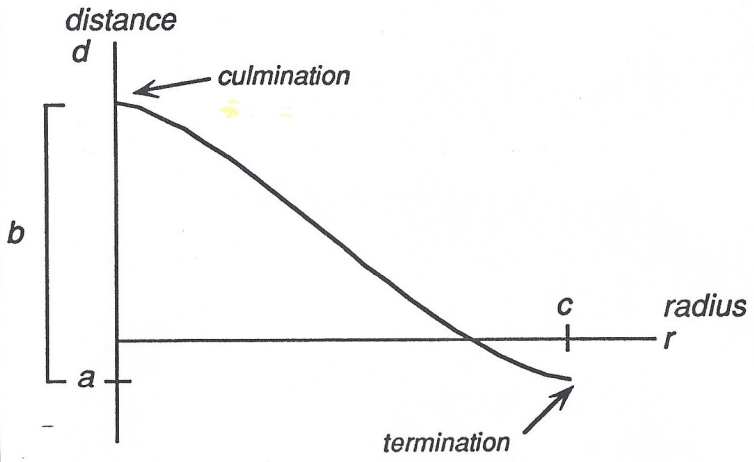

Figure 16. Parameter definitions for least-squares curve-fitting.

Ratliff, R.A., 1994, Three-Dimensional Fault-Propagation Folding: a Model Based on Displacement Variation. Journal of Structural Geology.

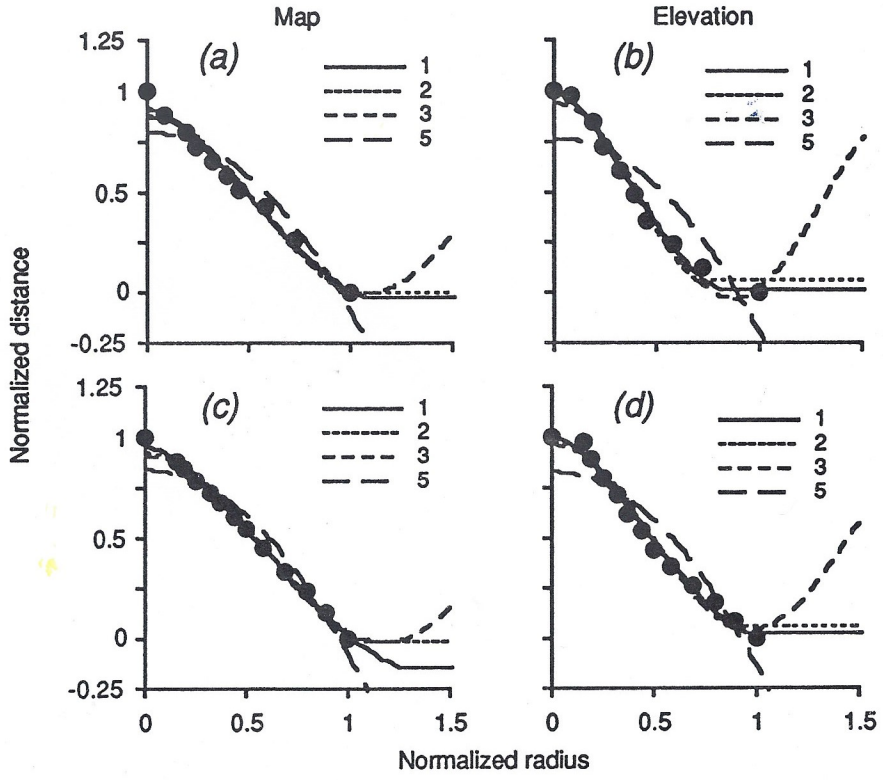

Figure 17. Map and elevation projections and best-fit analytic curve solutions for Frannie North (a) and (b) and Frannie South (c) and (d) hinge lines (see Fig. 15). Curves: 1, linear-arithmetic; 2, constant-arithmetic; 3, cosinusoidal; 5, parabolic. The linear-arithmetic curve is best-fitting solution for each projection, with no convergence for elliptical functions.

Table 6. Results of least-squares curve-fitting for different functions.

	Analytical curve	[1] χ^2 Mean	Median	Minimum	Maximum	[2] n
Map projection	Linear-arithmetic	0.0272	0.0110	0.0000	0.3728	91
	Constant-arithmetic	0.0315	0.0119	0.0001	0.3867	115
	Cosinusoidal	0.0295	0.0130	0.0001	0.2308	117
	Elliptical	0.0513	0.0240	0.0002	0.6883	68
	Parabolic	0.1006	0.0561	0.0004	0.8616	195
Elevation projection	Linear-arithmetic	0.0088	0.0048	0.0000	0.0816	98
	Constant-arithmetic	0.0099	0.0062	0.0000	0.0912	124
	Cosinusoidal	0.2344	0.0061	0.0000	29.4626	132
	Elliptical	0.0149	0.0078	0.0000	0.0678	60
	Parabolic	0.2003	0.0298	0.0001	29.5084	195

[1] $\chi^2 = \sum_{i=1}^{n} (y_i - \hat{y}_i)^2$, y_i and $\hat{y}_i$ are the observed and predicted displacement values, respectively.

[2] Number of convergent least-squares solutions.

Ratliff, R.A., 1994, Three-Dimensional Fault-Propagation Folding: a Model Based on Displacement Variation. Journal of Structural Geology.

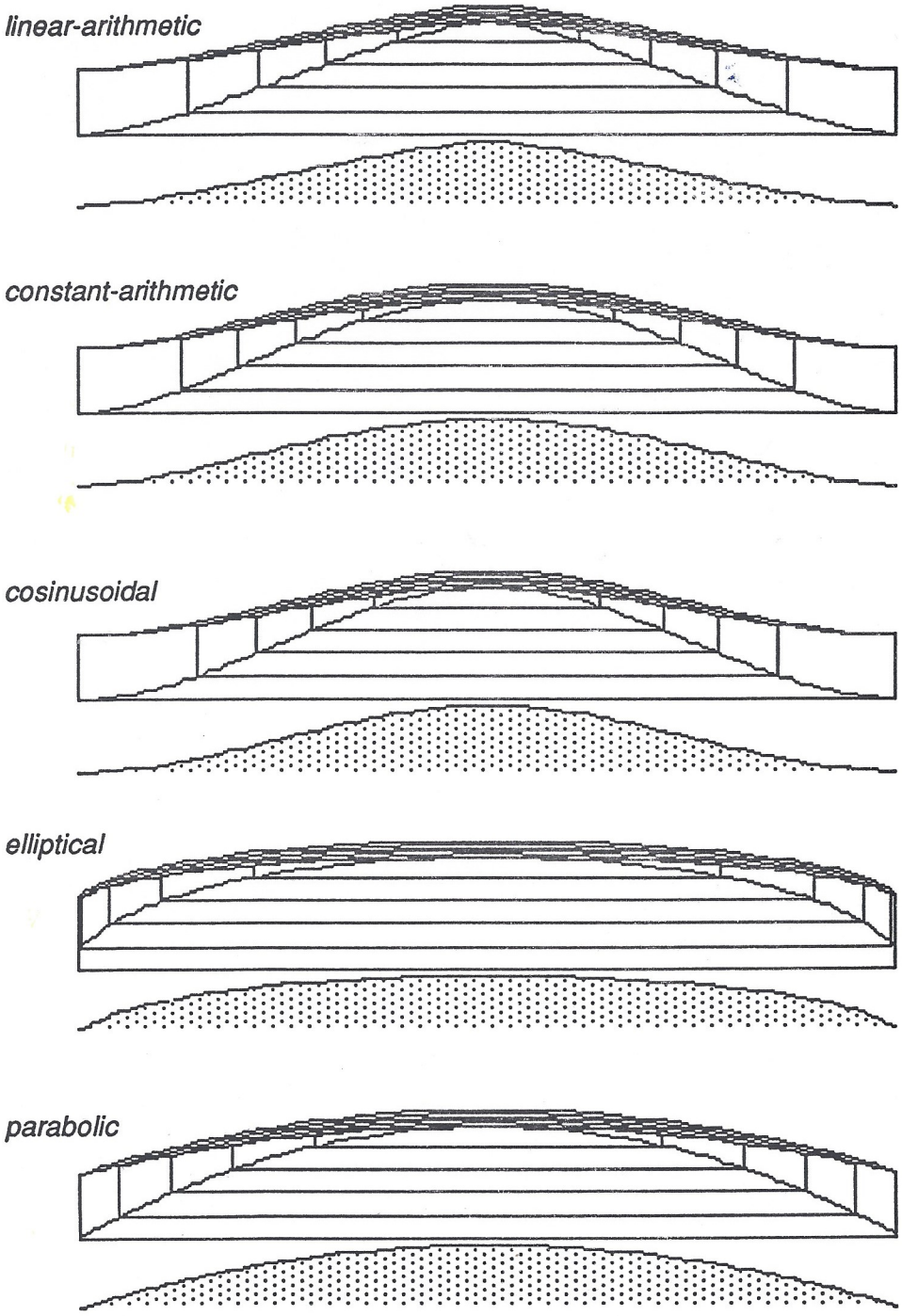

Figure 7(b). Contour maps and trailing-edge displacement profiles for 29°-ramp fault-propagation folds generated by various displacement functions. Fault parameters correspond to 5 km maximum displacement stage of Table 5. Contour interval 1 km.

Ratliff, R.A., 1994, Three-Dimensional Fault-Propagation Folding: a Model Based on Displacement Variation. Journal of Structural Geology.

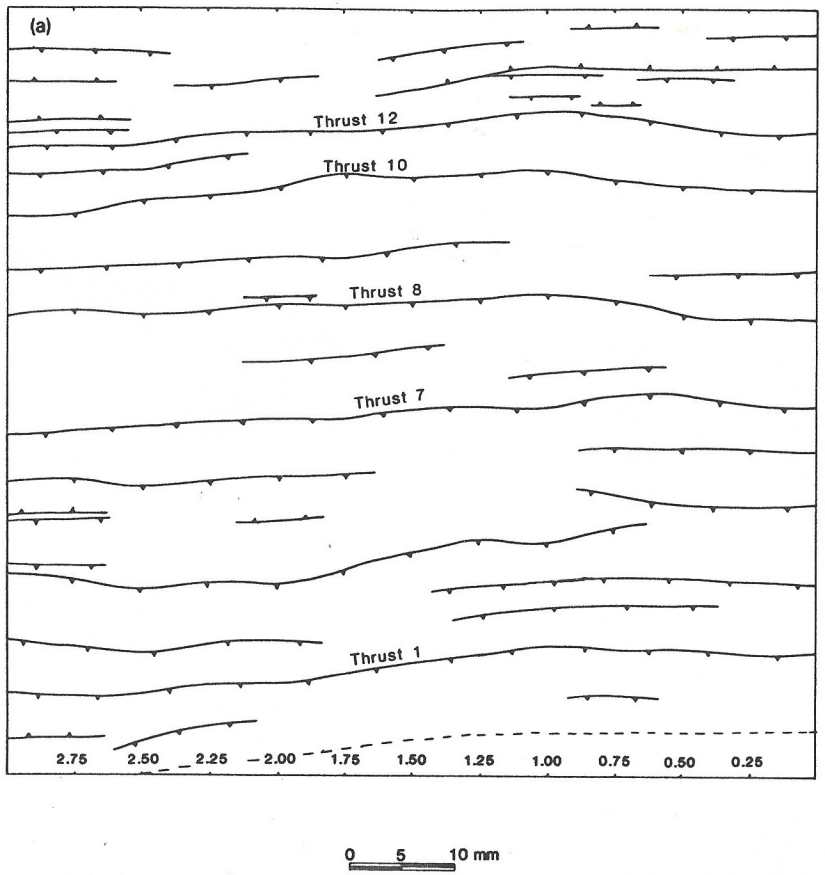

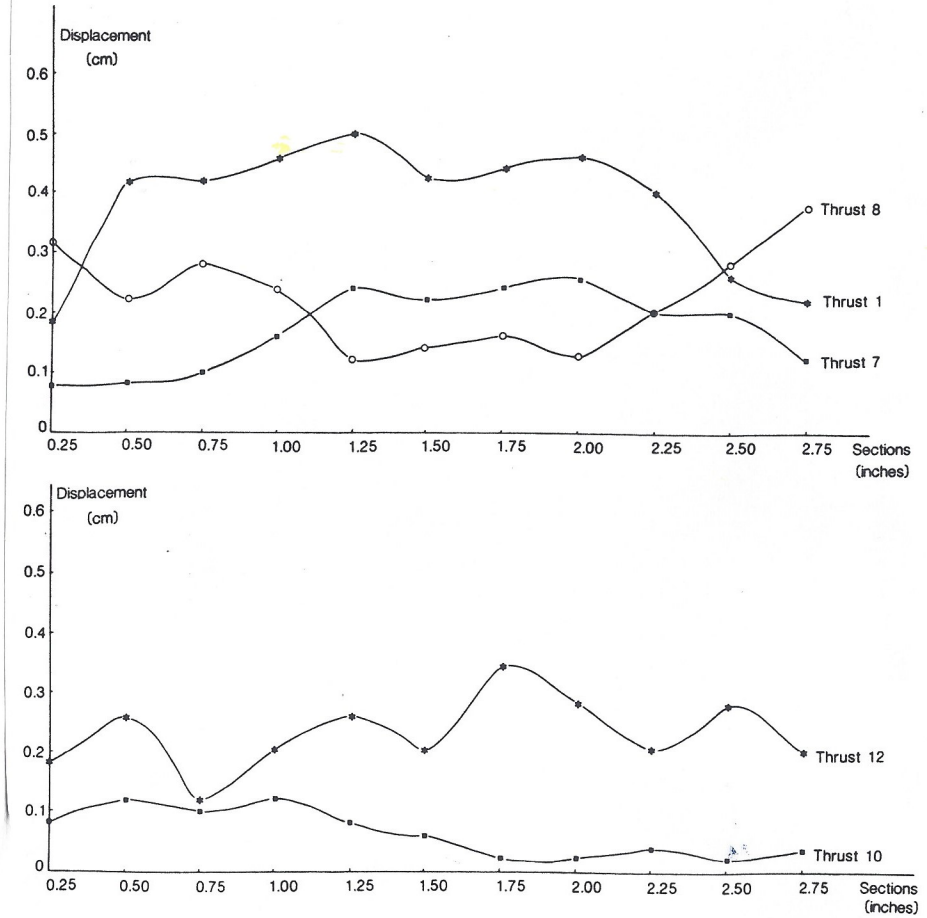

Fig. 11. Along-strike variation of thrust displacement for five thrusts in unit V, model TH-22.

Liu, S. and Dixon, J.M., 1991. Centrifuge modelling of thrust faulting: structural variation along strike in fold-thrust belts. *In*: P.R. Cobbold (Editor), Experimental and Numerical Modelling of Continental Deformation. Tectonophysics, 188: 39-62.

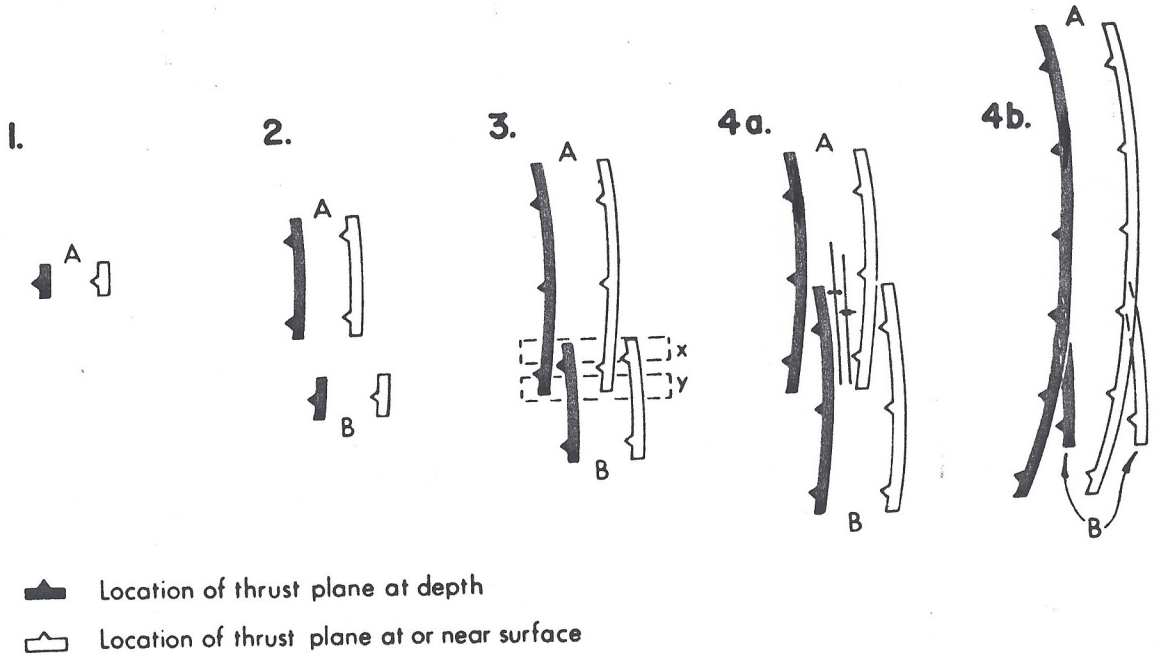

FIG. 10.—Diagram of show time and space relations between successive thrusts (plan view). **1.** Initial break of thrust A. **2.** Movement of A, initial break of thrust B. **3.** Movement of A and B. At X, thrust A is older than B. At Y, thrust A is younger than B. **4a.** Movement of thrust A ceases. Continued movement of B causes folding of thrust A. **4b.** Movement of B ceases. Continued movement of A causes it to override B.

LATERAL FAULT CAPTURE

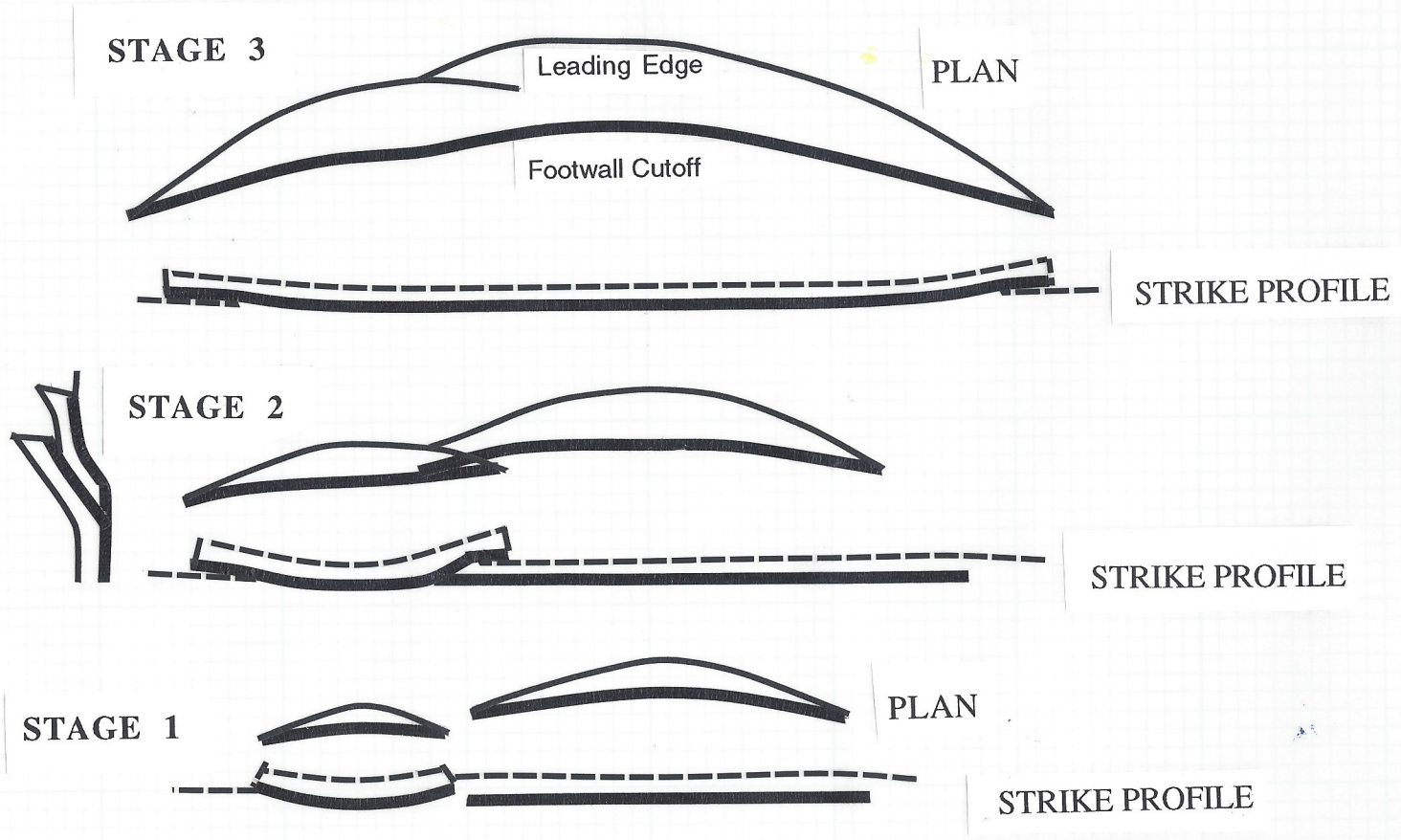

NORMAL LATERAL CAPTURE

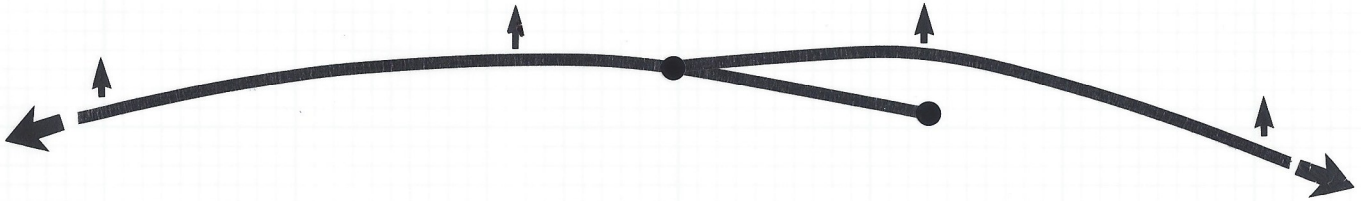

"OUT-OF-SEQUENCE" PROPAGATION

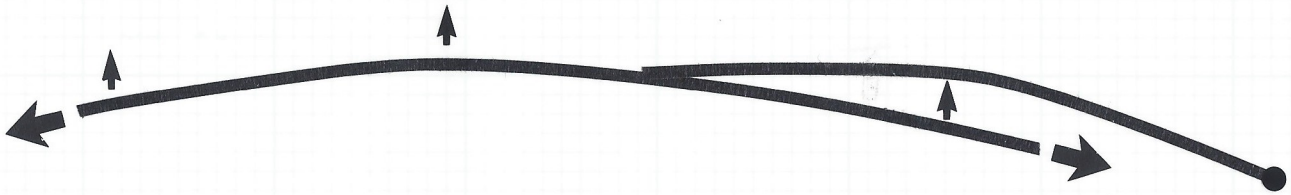

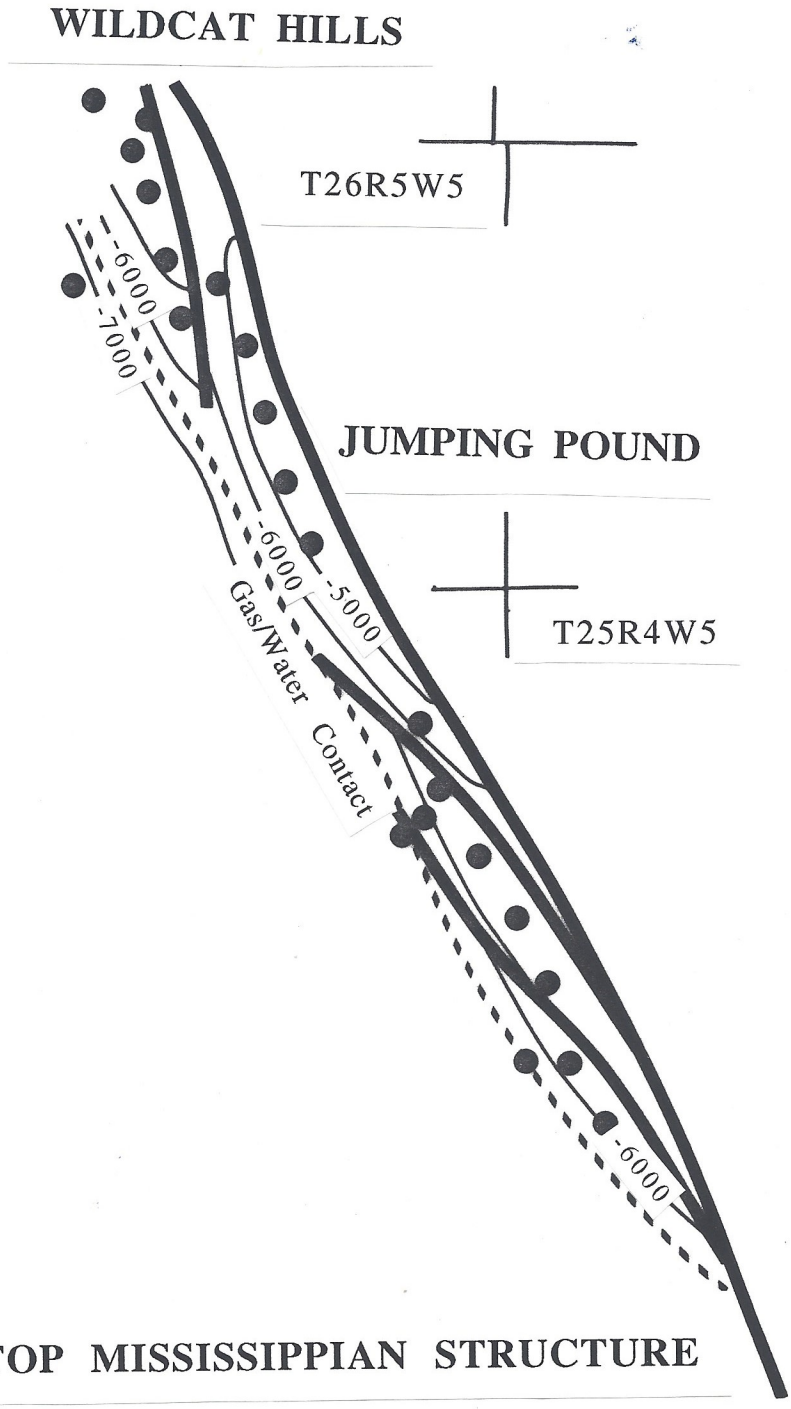

TOP MISSISSIPPIAN STRUCTURE

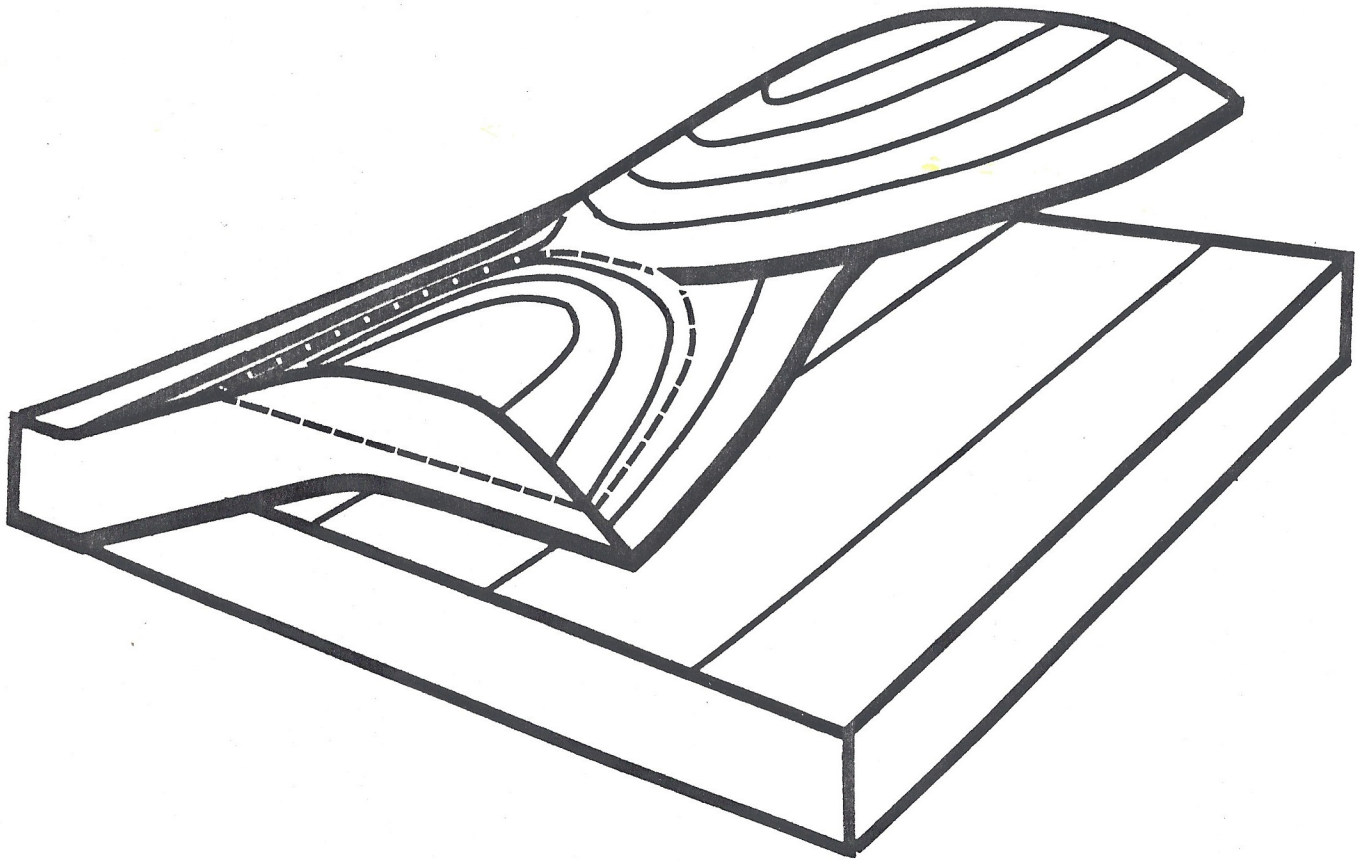

TRAP FILL LEVEL CONTROLLED BY LEAK POINT
ALONG FAULT NETWORK